Title

Localization of complement factor H gene expression and protein distribution in the mouse outer retina.

Authors

Smit-McBride, Zeljka
Oltjen, Sharon L
Radu, Roxana A
et al.

Publication Date

2015

Peer reviewed

Molecular Vision 2015; 21:110-123 <http://www.molvis.org/molvis/v21/110>
Received 30 June 2014 | Accepted 3 February 2015 | Published 5 February 2015

Localization of *complement factor H* gene expression and protein distribution in the mouse outer retina

Zeljka Smit-McBride,[1] Sharon L. Oltjen,[1] Roxana A. Radu,[2] Jason Estep,[3] Anthony T. Nguyen,[1] Qizhi Gong,[3] Leonard M. Hjelmeland[1]

[1]Department of Ophthalmology, University of California, Davis, CA; [2]Jules Stein Eye Institute, University of California, Los Angeles, CA; [3]Department of Human Anatomy and Cell Biology, University of California, Davis, CA

Purpose: To determine the localization of complement factor H (Cfh) mRNA and its protein in the mouse outer retina.
Methods: Quantitative real-time PCR (qPCR) was used to determine the expression of Cfh and Cfh-related (Cfhr) transcripts in the RPE/choroid. In situ hybridization (ISH) was performed using the novel RNAscope 2.0 FFPE assay to localize the expression of Cfh mRNA in the mouse outer retina. Immunohistochemistry (IHC) was used to localize Cfh protein expression, and western blots were used to characterize CFH antibodies used for IHC.
Results: Cfh and Cfhr2 transcripts were detected in the mouse RPE/choroid using qPCR, while Cfhr1, Cfhr3, and Cfhrc (Gm4788) were not detected. ISH showed abundant Cfh mRNA in the RPE of all mouse strains (C57BL/6, BALB/c, 129/Sv) tested, with the exception of the $Cfh^{-/-}$ eye. Surprisingly, the Cfh protein was detected by immunohistochemistry in photoreceptors rather than in RPE cells. The specificity of the CFH antibodies was tested by western blotting. Our CFH antibodies recognized purified mouse Cfh protein, serum Cfh protein in wild-type C57BL/6, BALB/c, and 129/Sv, and showed an absence of the Cfh protein in the serum of $Cfh^{-/-}$ mice. Greatly reduced Cfh protein immunohistological signals in the $Cfh^{-/-}$ eyes also supported the specificity of the Cfh protein distribution results.
Conclusions: Only *Cfh* and *Cfhr2* genes are expressed in the mouse outer retina. Only Cfh mRNA was detected in the RPE, but no protein. We hypothesize that the steady-state concentration of Cfh protein is low in the cells due to secretion, and therefore is below the detection level for IHC.

The discovery that the human *CFH* Y402H allele is associated with the risk for developing age-related macular degeneration (AMD) initiated the modern study of the genetics of this disease [1-6]. The *CFH* gene (Gene ID: 3075, OMIM: 134370) encodes for complement factor H, one of the regulators of the alternative pathway of the complement activation system. This discovery also shed light on the complement system and its dysfunction as a possible role for the development of AMD. It is now clear that AMD is much like other complex genetic diseases in that susceptibility develops as a function of age, genetics, and non-genetic influences [7].

The use of the mouse as an animal model has been explored as a reasonable alternative to working with human specimens for the study of *Cfh* genetics and phenotypes [8-10]. The mouse and human *CFH* gene clusters are similar but not identical. Experimental comparisons at every level of detail from the structure of the gene cluster to the physiology of the entire complement system have not been fully explored. The best clarification of the relative structures of the mouse and human *CFH* gene clusters, at the levels of nucleotide and amino acid sequence and the relative homology of *CFH* and its related genes within the two species, can be found in an article by Hellwage et al. [11].

Despite high interest in understanding complement factor H function in the eye, total agreement has not yet been achieved regarding which cells in the outer retina express the Cfh message and the nature of the protein distribution. Several studies report the expression of *Cfh* and *Cfh*-related genes in the retina and RPE of the posterior pole in the mouse [12,13]. One study found Cfh protein only in Bruch's membrane of the mouse eye [14]. Another study reported Cfh protein in the mouse photoreceptor sensory cilium complex [15]. The literature referenced outlines only potential problems when comparing mouse and human *CFH* genes. Many investigators have explored the distribution of mouse complement factor H using antibodies generated against human complement factor H as the antigen [13,14,16,17]. In particular, most of the antibody reagents used do not have clear references for the host organism, the exact identity of the antigen used, and the state of antibody purification of the final product. Frequently, the term "affinity purified" used in publications may mean only an isolated immunoglobulin G (IgG) fraction.

In this work, we reexamined the expression of the *Cfh* gene cluster in the mouse RPE/choroid using a full set of quantitative real-time PCR (qPCR) assays for all genes in the mouse *Cfh* cluster. Cells that synthesize Cfh mRNA

Correspondence to: Leonard M. Hjelmeland, University of California Davis, School of Medicine, Vitreoretinal Research Lab, Davis, CA, 95616; email: lmhjelmeland@ucdavis.edu

were identified using a novel in situ hybridization (ISH) method with probes specifically designed to not cross-react with related genes. We also investigated the distribution of complement factor H in the outer retina and RPE using two antibodies that were raised against mouse-specific protein sequences. Finally, we investigated a freeze substitution protocol to improve the preservation of structure and antigenicity in the outer retina.

METHODS

Animals: Male BALB/c and C57BL/6 mice were purchased from the Jackson Laboratory (Bar Harbor, ME). Eyes from *129/Sv Cfh*$^{-/-}$ mice (5 1/2 months of age) and their background strain 129/Sv (6 months of age) were a gift from Dr. R. Radu (Jules Stein Eye Institute, UCLA). Mice were provided with water and standard chow (Rodent Diet 5001, PMI Feeds, Inc., Shoreview, MN) ad libitum and maintained on a 12 h:12 h light-dark cycle. All animals were handled and housed according to the ARVO Statement for the Use of Animals in Ophthalmic and Vision Research. This research was conducted according to protocols approved by the Institutional Animal Care and Use Committee at the University of California, Davis.

RNA isolation and quantitative real-time PCR: Eyes were collected, immobilized to a Petri dish using superglue, and quickly dissected by a circumferential cut posterior to the limbus. The retina was removed and the RPE/choroid dissected out and placed in 300 µl of RNAlater (Ambion, Life Technologies, Grand Island, NY) within a minute, following our previously published rapid dissection procedure [18]. Tissue was stored at −20 °C until subsequent processing.

Total RNA from the RPE/choroid tissue samples were extracted and purified using the Qiagen RNeasy isolation kit (Qiagen, Valencia, CA) following the manufacturer's protocol. The quantity and quality of total RNA from each sample was analyzed using the Agilent 2100 BioAnalyzer and RNA 6000 Nano Kit (Agilent, Santa Clara, CA).

qPCR experiments were performed using total RNA isolated from the RPE/choroid of 2 month old mice with biologic replicates of n=6 (3 males and 3 females), for a total of six animals. qPCR was also performed on the 129/Sv and *129/Sv Cfh*$^{-/-}$ strains using biologic replicates (n=2 males and n=4 females), for a total of six animals. Each biologic replicate was run in triplicate. The reverse transcription of mRNA was performed using the QuantiTect Reverse Transcription Kit (Qiagen). The following TaqMan assays (Applied Biosystems by Life Technologies, or ABI) were performed for qPCR: mouse *Cfh* (ABI No. Mm01299243_m1) [ABI part of Life Technologies, Grand Island, NY], mouse *Cfhr1* (ABI No. Mm01295946_m1), mouse *Cfhr2* [Cfhrb_4/2 (ABI No. Mm03040548_m1)], mouse *Gm4788* [Cfhrc (ABI No. Mm02581433_mH)], mouse *Cfhr3* custom made, and three reference genes, *B2mex* (Mm00437762_m1), *Gapdh* (ABI No. Mm03302249_g1), and *Hprt* (ABI No. Mm01545399_m1).

Tissue processing for immunohistochemistry and in situ hybridization: Animals were sacrificed by asphyxiation with gaseous CO_2 in a closed chamber. For orientation in paraffin, the superior region of each eye was marked using tissue dye (The Davidson Marking System, Bradley Products Inc., Bloomington, MN, catalog #1003–6) before enucleation with curved scissors. Eyes were fixed using one of two methods. In the first method, the whole globe was immersed in freshly prepared 10% neutral buffered formalin overnight after enucleation and subsequently used for in situ hybridization. Eyes to be used for immunohistochemistry (IHC) were fixed using a second fixation method involving freeze substitution. Each excised eye was snap frozen in dry ice–cooled liquid propane for 30 s, and then transferred to dry ice–cooled methanol containing 3% glacial acetic acid. Eyes immersed in this fixative were kept at −80 °C for 48 h, followed by overnight at −20 °C, after which they were embedded in paraffin as follows: Eyes were warmed to room temperature and left for 1–2 h in 100% ethanol, 2×30 min in 100% ethanol, 2×15 min in xylene, and 3×40 min in paraffin.

Each eye was placed in a paraffin mold in an orientation-specific manner. First, the eye was manipulated so that the previous corneal marking was in the 12 o'clock position. Next, the eye was rotated so that the anterior segment faced the right side of the mold before the embedding ring was placed on top, thus preserving the orientation of the eye, such that when the mold was released from the block, the superior orientation was maintained and a sagittal section made of the eye when the block was sectioned. Sections were cut using a Leica RM2125RT microtome (Leica, Nussloch, Germany) at 6 µm. Due to the previous orientation of each eye in the paraffin embedding step, a section through the optic disc represented a sagittal section.

In situ hybridization: In situ hybridization was performed using a mouse *Cfh* probe (catalog, #403671, Advanced Cell Diagnostics [ACD]; Hayward, CA) specific to the *Cfh* (Accession #NM_009888.3) sequence region spanning 2131–3109 bp, and the novel RNAscope 2.0 FFPE Fast Red Assay (ACD) as directed by the manufacturer [19] with the following modifications: Pretreatment 2 was optimized for each set of eyes processed for ISH, the Amp 5 step was reduced to 20 min, and the hematoxylin staining time was reduced to 2×2 s. Briefly, paraffin was removed from 6-µm-thick sections using xylene, followed by dehydration in 100% ethanol

before the slides were dried at room temperature. Endogenous peroxidase activity was blocked before the slides were boiled in Pretreatment 2, followed by treatment with protease, and hybridization with the target oligo probes (ACD). After hybridization, a six-step amplification process (preamplifier, signal enhancer, amplifier, label probe, signal amp, AP-linked labeling) was performed before chromogenic detection using Fast Red. Slides were then counterstained with Gill's hematoxylin, dehydrated, and coverslipped using EcoMount mounting media (Biocare Medical, Concord, CA). Specific ISH signals appeared as punctate red spots. An RPE65 probe was used as a positive control, and a bacterial dapB probe was used as a negative control.

Antibodies: Goat anti-mouse Cfh and rabbit anti-mouse Cfh primary antibodies (Santa Cruz Biotechnology, Santa Cruz, CA) were used, along with their appropriate secondary antibody (biotinylated bovine anti-goat IgG or cyanine 3 (Cy3) conjugated donkey anti-goat IgG; or biotinylated donkey anti-rabbit IgG) for immunohistochemistry (Jackson ImmunoResearch, West Grove, PA). Alkaline phosphatase conjugated secondary antibodies (Jackson ImmunoResearch) were used for western blots. See Table 1 for a summary of the antibodies used.

Western blots: Purified human CFH protein (Complement Technology, Inc., Tyler, TX), mouse complement factor H (gift from Dr. Claire Harris, Cardiff University), C57BL/6 mouse serum (1 µl/lane; Bioreclamation LLC, Westbury, NY), and mouse serum from 129/Sv and *129/Sv Cfh*$^{-/-}$ (1 µl/lane; gift from Dr. Roxana Radu, Jules Stein Eye Institute, UCLA) samples were prepared in sample buffer (Bio-Rad, Hercules, CA, catalog #NP0007) with beta mercaptoethanol. All samples were electrophoresed on 4–15% Tris-HCl gradient gels (Bio-Rad Criterion gels), after which the protein bands were transferred onto polyvinylidene fluoride (PVDF; Bio-Rad, catalog #162–0174) membranes, and blocked overnight with 5% nonfat dry milk (EMD Millipore, Billerica, MA, catalog #6250) in Tris buffered saline containing 0.05% Tween-20 (TBST).

For immunolabeling of western blots, primary antibodies were diluted (1 µg/ml) in TBST containing 5% nonfat dry milk, incubated 1 h at room temperature, washed in TBST, and incubated for 1 h at room temperature in species-specific secondary antibodies conjugated to alkaline phosphatase (AP) diluted 1:40,000 in TBST. Blots were washed before developing in BCIP/NBT substrate (Vector Laboratories, Burlingame, CA, catalog #SK-5400). After development, the blots were washed in ultrapure water and air dried in the dark.

Immunohistochemistry: Paraffin sections were placed on SuperFrost Plus microscope slides and dried overnight at room temperature. Sections from freeze-substituted tissue were deparaffinized in xylene and hydrated through gradient alcohols, washed in PBS (1X; 137 mM NaCl, 2.7 mM KCl,

Table 1. Antibodies, suppliers, and concentrations used for immunohistochemistry and western blots.

Primary Antibody and Concentration Used (Manufacturer & catalog #)	Host Species	Immunogen	Secondary Antibody (Manufacturer & catalog #)
anti-mouse Factor H, affinity purified polyclonal, 2 ug/ml (IHC-P), 1 ug/ml (WB); (Santa Cruz Biotechnology, catalog # 17951)	goat	Peptide mapping within an internal region of Factor H of mouse origin (aa 250–300)	Biotinylated bovine anti-goat IgG (Jackson ImmunoResearch, catalog # 805–065–180) Cy3 donkey anti-goat IgG (Jackson ImmunoResearch, catalog # 705–165–147) Alkaline Phosphatase conjugated bovine anti-goat IgG (Jackson ImmunoResearch, catalog #805055180)
anti-mouse Factor H, recombinant polyclonal, 6 ug/ml (IHC-P), 1 ug/ml (WB), (Santa Cruz Biotechnology, catalog # 33157)	rabbit	Amino acids 61–360 mapping within an internal region of Factor H of mouse origin	Biotinylated donkey anti-rabbit IgG (Jackson ImmunoResearch, catalog # 711–065–152) Alkaline Phosphatase goat anti-rabbit IgG (Jackson ImmunoResearch, catalog #111055003)
anti-Rhodopsin, clone 4D2, monoclonal antibody, 1:500, (Millipore, catalog # MABN15)	mouse	Rat rod outer segments corresponding to rat Rhodopsin at the N-terminus	Cy2 conjugated donkey anti-mouse IgG, 1:100 (Jackson ImmunoResearch, catalog #715–225–150)
anti-Opsin, Blue, polyclonal, 1:500, (Millipore catalog # AB5407)	rabbit	Recombinant human blue opsin	Cy5 conjugated donkey anti-rabbit IgG, 1:100 (Jackson ImmunoResearch, catalog #711–175–152)
anti-Opsin, Red/Green, 1:500, polyclonal, (Millipore catalog # AB5405)	rabbit	Recombinant human red/green opsin	Cy5 conjugated donkey anti-rabbit IgG, 1:100 (Jackson ImmunoResearch, catalog #711–175–152)

8 mM Na_2HPO_4, and 2 mM KH_2PO_4, pH 7.4; Ambion, Grand Island, NY, catalog #AM9625), and post fixed in 4% paraformaldehyde in PBS, pH 7.4 for 10 min and washed again with PBS. Antigen retrieval was performed at 98 °C using 1X Dako Target Retrieval Solution (DakoCytomation, Carpinteria, CA, catalog #S1699) for 20 min and left at room temperature for 20 min before washing with PBS. Finally, the slides were blocked using 3% BSA in PBS buffer for 2 h at room temperature.

Primary antibody binding was performed overnight at 4 °C. Antibodies were diluted to a specific concentration in their blocking buffer. After primary antibody exposure, sections were washed in PBS containing 0.1% Tween-20, and then incubated with the appropriate biotinylated secondary antibody at a concentration of 6 µg/ml diluted in PBS containing 0.05% Tween-20 for 30 min, washed, and incubated for 30 min in Vectastain ABC-AP reagent (Vector Laboratories, catalog #AK-5000). The secondary antibodies were evaluated for non-specific labeling using primary antibody deletion or an isotype-matched immunoglobulin at the same concentration as the primary antibody. Color was developed using the BCIP/NBT alkaline phosphatase (AP) substrate (Vector Laboratories, catalog #SK-5400). The slides were then washed, counter-stained with Nuclear Fast Red (Vector Laboratories, catalog #H-3403), washed again, dehydrated, cleared in xylene, and coverslipped using Vecta-Mount permanent mounting media (Vector Laboratories, catalog #H-5000).

Immunofluorescent labeling was performed as described above until the blocking step. Immunofluorescent blocking buffer contained 5% normal donkey serum (Jackson ImmunoResearch) and 0.3% Triton X-100 (Sigma, St. Louis, MO, catalog #T8787) in PBS. After blocking with immunofluorescent blocking buffer, the slides were incubated overnight at 4 °C with appropriate primary antibodies diluted in PBS containing 0.3% Triton X-100 (Sigma Aldrich, Saint Louis, MO). After incubation with primary antibodies, the slides were washed with PBS and incubated for 30 min at 37 °C with the appropriate fluorescent labeled secondary antibodies diluted in PBS and washed before coverslipping. Fluoromount G with 4',6-diamidino-2-phenylindole (DAPI) mounting media (SouthernBiotech, Birmingham, AL, catalog #0100–20) was used to coverslip slides.

Double-labeling experiments for Cfh with either fluorescein conjugated wheat germ agglutinin (WGA) or peanut agglutinin (PNA; both from Vector Laboratories, catalog #FL-1021 and #FL-1071, respectively) were performed using eyes from male C57BL/6 mice. Eyes were fixed using the freeze substitution method and embedded in paraffin as described above. However, these eyes were oriented for coronal rather than sagittal sections. The posterior portion of the eye was oriented such that it was on the cutting face of the paraffin block. Sections from the posterior region of the eye were cut at 6 µm and dried overnight at room temperature. Briefly, double labeling was performed as follows: The paraffin was removed in xylene, hydrated through gradient alcohols, and washed in PBS. Sections were then post-fixed in 4% paraformaldehyde for 10 min before being subjected to antigen retrieval at 98 °C for 20 min in 1X Dako Target Retrieval Solution (DakoCytomation, catalog #S1699). After antigen retrieval, the slides were left at room temperature for 20 min before washing with PBS containing 0.3% Triton X-100. Slides were then blocked for 1 h at 37 °C with PBS containing 0.3% Triton X-100 and 5% normal donkey serum. The slides were then incubated overnight at 4 °C in a humidity chamber with 0.8 µg/ml goat anti-mouse Cfh antibody and either 15 µg/ml PNA or 5 µg/ml WGA, both lectins conjugated to fluorescein (Vector Laboratories). The next morning, the slides were washed with PBS and incubated for 30 min at 37 °C in a humidity chamber with Cy3 conjugated donkey anti-goat IgG (Jackson ImmunoResearch, catalog #705–165–147), and coverslipped using Fluoromount G with DAPI (SouthernBiotech) mounting media before visualizing using an Olympus FluoView FV1000 confocal microscope (Olympus America, Inc., Center Valley, PA).

Antibody blocking experiments are used to demonstrate specificity in IHC. The lowest goat anti-mouse Cfh antibody concentration for IHC was determined and preabsorbed using the manufacturer's protocol and blocking peptide (Santa Cruz Biotechnology, catalog #17951 P) for this antibody. Briefly, the antibody was combined with a fivefold excess of blocking peptide in PBS to a final volume of 500 µl and incubated overnight on a rocker at 4 °C. The preabsorbed antibody was diluted and used for IHC at the same concentration as the non-absorbed antibody (2 µg/ml).

Photography: Slides were viewed and digitized images captured using a light microscope (Nikon Eclipse E800; Nikon Inc., Melville, NY) and epifluorescence with an AF568 filter (Nikon Set 49,005) using QCapture software (QImaging, Surrey, Canada).

RESULTS

Structural comparison of human and mouse Cfh gene clusters and proteins: To compare the organization between the human and mouse *Cfh* gene clusters, at the gene and protein levels, we used the UC Santa Cruz Gene Browser. The best reference in the literature for discussing a comparison of the mouse and human *CFH* gene clusters and associated proteins

is the Hellwage et al. paper [11]. The order of genes in the human versus the mouse complement clusters is shown in Figure 1. The human *CFH* cluster is located on human chromosome 1 within the 360 kb interval located within the 196-197 Mbp region of Chr1, according to the human genome assembly from Feb 2009 (GRCh37/hg19). The cluster is located on the "+" strand of chromosome 1, and thus directed in the "+" direction. The cluster of mouse *Cfh* genes is located on chromosome 1, within the 670 kb interval located within the 140-142 Mbp region of Chr1, according to the UCSC Genome Browser, mouse genome assembly from Dec 2011 (GRCm38/mm10). The cluster is located on the "-" strand of chromosome 1 and thus directed in the "-" direction. Note that the order of genes in the cluster is different for the mouse and human. In the human cluster, the *CFH* gene is followed by *CFHR3*, *CFHR1*, *CFHR4*, *CFHR2*, and the last one is *CFHR5*. In the mouse cluster, *Cfhr2* is located immediately downstream of the *Cfh* gene followed by *Gm4788*, *Cfhr3*, and *Cfhr1*. In the human, there is evidence of the expression of all six genes mainly in the liver [20]. The simultaneous expression of *CFH*, *CFHR3*, and *CFHR1* has been proposed to have functional significance in the pathogenesis of AMD [21]. However, no evidence for the expression of the *Cfhr3* and *Cfhr1* genes has been found thus far in the mouse eye.

Transcripts for the *Cfh* gene cluster in the mouse were first identified in 1990 [22]. Sixteen years later, two transcripts were shown to code for two proteins that were expressed [11]. These proteins were termed complement factor H-related B (FHR-B) and complement factor H-related C (FHR-C). With the full sequencing of the mouse genome, it became clear that there are four potential *Cfh*-related genes in the mouse as opposed to five related genes in the human. Since various names have historically been used for *Cfh* and *Cfh*-related genes and their corresponding proteins, we have included a table in the Appendix for the synonyms of these genes and their proteins (Appendix 1).

The *Cfh* gene is composed of 20 short consensus repeats (SCR) or Sushi domains [11]. SCRs within one gene have variable homologies. When mouse and human *CFH* sequences are compared, the extent of the non-homology of the SCR repeats can be easily determined (Figure 2).

Quantification of expression levels of Cfh and Cfhr2 mRNA in the RPE/choroid with qPCR: To have a quantitative accounting of all possible transcripts from the mouse *Cfh* gene cluster, we performed qPCR analysis on the RNA samples derived from the RPE/choroid of the mouse. Primers for all *Cfh*-related genes were not commercially available, and as a result, we had ABI develop a custom qPCR TaqMan assay for mouse *Cfhr3*. The qPCR studies were performed using qPCR TaqMan assays (ABI) for all mouse *Cfh* and *Cfhr* genes that were designed to not cross-react with other members of the family.

qPCR was performed on the RPE/choroid from male (n=3) and female (n=3) C57BL/6 mice at 2 months of age for Cfh, Cfhr1, Cfhr2 (Cfhrb_4/2), Cfhr3, and Gm4788 (Cfhrc). Only Cfh and Cfhr2 were expressed in the RPE/choroid (Figure 3A). No gender-related difference in expression was observed (data not shown). The other related mRNAs were not detected. When qPCR was performed on the RPE/choroid from the *129/Sv Cfh*$^{-/-}$ mice [23] and their age and background-matched wild-type mice (129/Sv), a strong Cfh signal was detected in the wild-type (WT) mice and low expression in the knockout mice (Figure 3B). The general level of expression of Cfhr2 mRNA was low in the wild-type strains, C57BL/6 and 129/Sv, compared to Cfh mRNA. Interestingly, we observed that Cfhr2 mRNA was significantly ($p<0.05$) upregulated in the *Cfh* knockout strain compared to the wild-type background strain (Figure 3C).

Localization of Cfh mRNA in RPE by ISH: To define the cell types in the posterior pole expressing Cfh transcripts, we performed in situ hybridization. The ISH results using the RNAscope 2.0 FFPE Assay are shown in Figure 4. In the RPE of the C57BL/6 and BALB/c mouse, the negative control

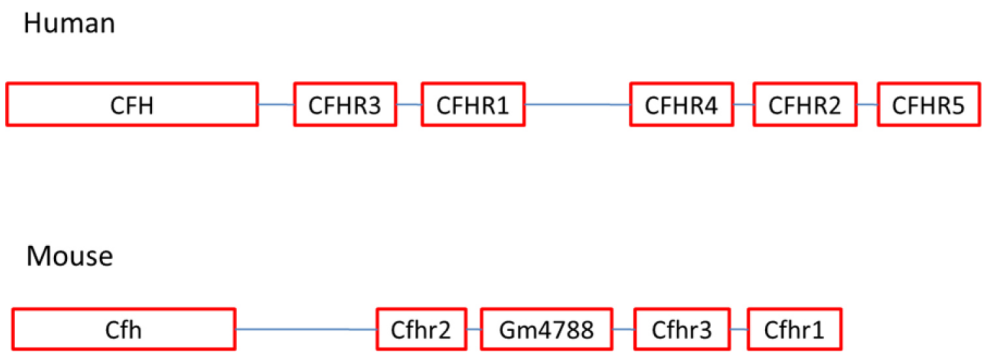

Figure 1. Comparison of *Cfh* gene clusters between the human and the mouse. Note the difference in the number of related genes expressed, as well as in their organization on the chromosome between the two species.

Figure 2. Comparison of the mouse and human complement factor H amino acid sequence and their SCR domains. Yellow denotes conserved amino acids, and green denotes homologous substitutions. Abbreviations: SCR=short consensus repeats; mCfh=mouse Cfh; hCFH=human CFH.

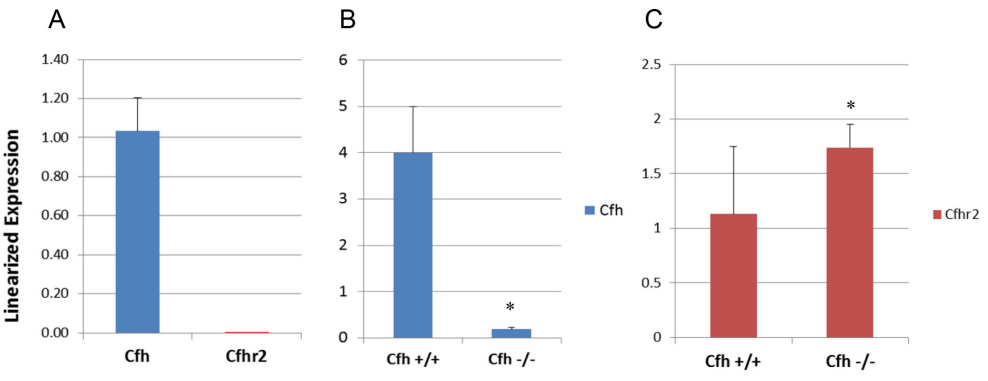

Figure 3. qPCR data for Cfh and Cfhr2 from the mouse RPE/choroid. Quantitative real-time PCR (qPCR) results are shown for RPE/choroid samples (n=6) from C57BL/6 mice for Cfh and Cfhr2 (**A**). Results for *129/Sv Cfh*$^{-/-}$ mice along with their wild-type background strain (129/Sv) are shown for Cfh (**B**) and Cfhr2 (**C**). Note that the *Cfh* message was still detected in the *Cfh*$^{-/-}$ mice, but at a low level. (*) denotes significant difference ($p<0.05$).

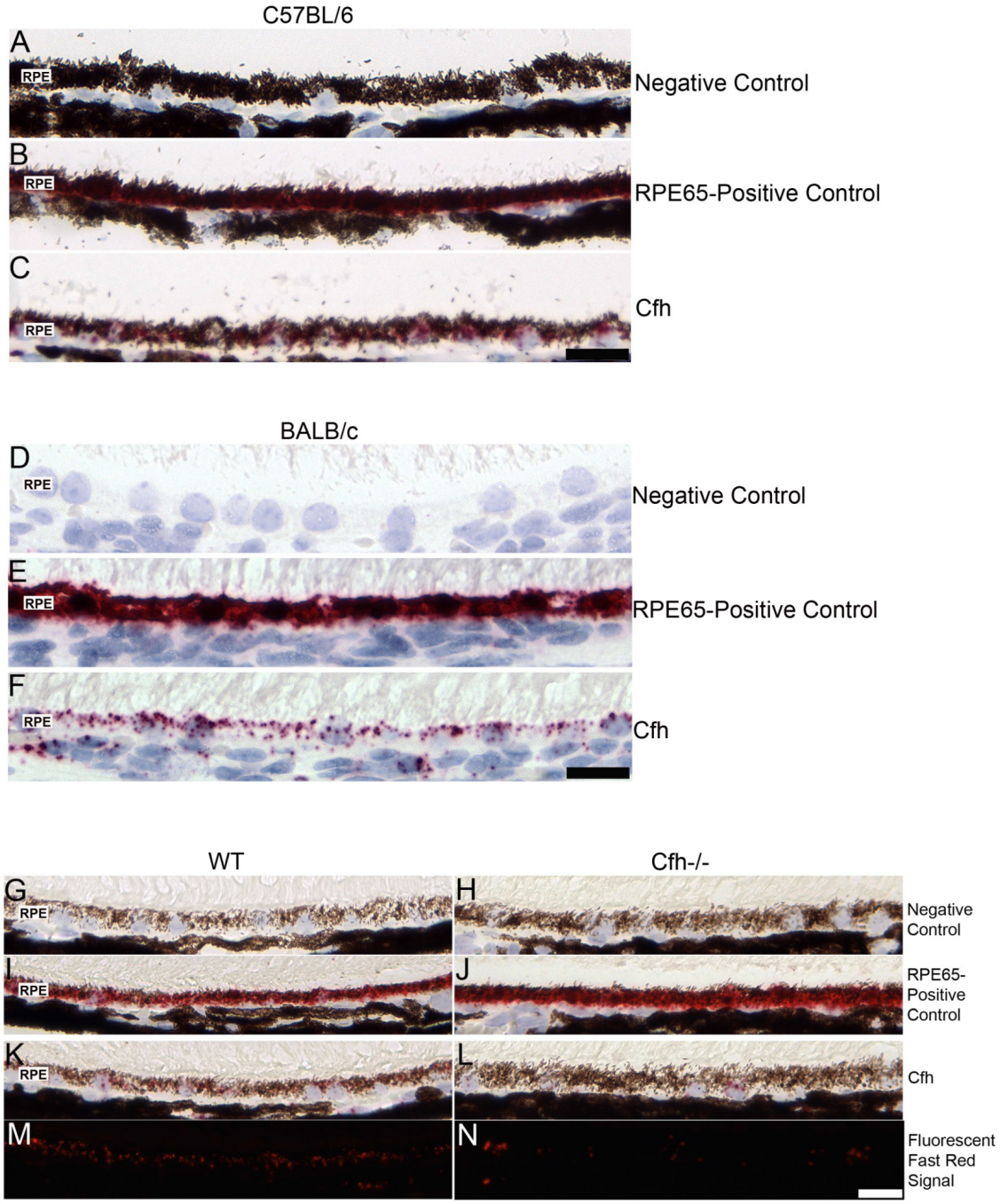

Figure 4. In situ hybridization in the C57BL/6, BALB/c, 129/Sv, and *129/Sv Cfh*$^{-/-}$ mouse eye. A C57BL/6 eye sectioned near the optic nerve with its negative control (**A**), RPE65 positive control (**B**), and Cfh probe (**C**) are shown. Similar in situ hybridization (ISH) results were observed in the BALB/c strain: negative control (**D**), RPE65 positive control (**E**), and Cfh probe (**F**). Note the robust Cfh mRNA signal in the RPE in both strains (Figure 4C,F). Negative and RPE65 positive controls and Cfh ISH results for a *129/Sv Cfh*$^{-/-}$mouse (**H**, **J**, **L**) and its background strain, 129/Sv (**G**, **I**, **K**) are shown. To visualize the Fast Red signal masked by the RPE pigment, the Fast Red fluorescence property was used to image the sections using a rhodamine filter for 129/Sv (**M**) and *129/Sv Cfh* $^{-/-}$ (**N**). Note the greatly reduced signal in the RPE of the *Cfh*$^{-/-}$ eye compared to the background strain. RPE=retinal pigment epithelium. Scale bar=20 µm.

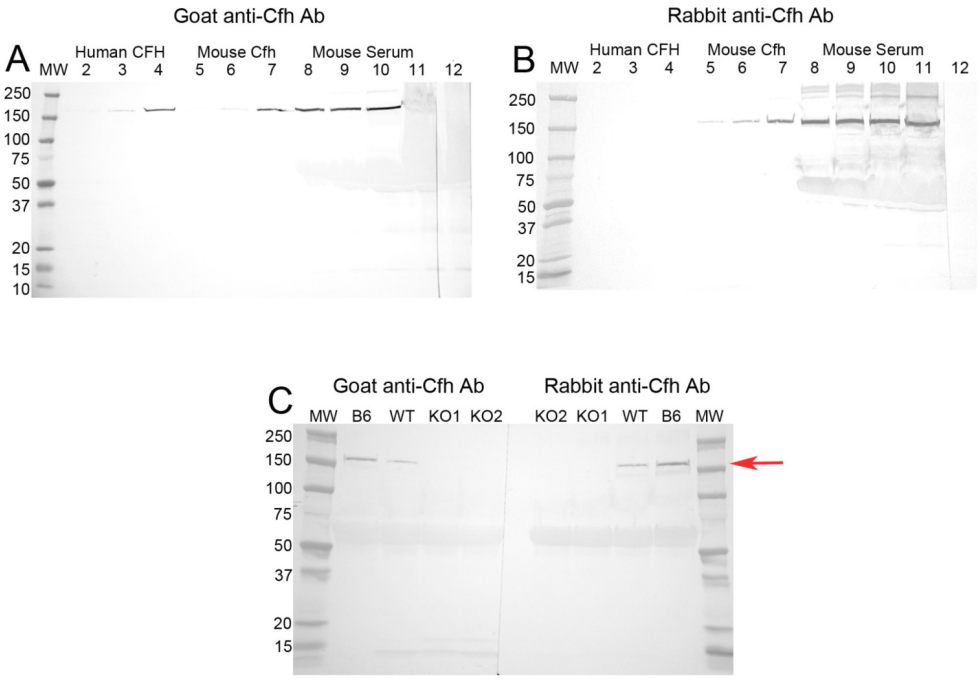

Figure 5. Western blots using different anti-mouse Cfh antibodies. Goat anti-mouse Cfh (**A**) and rabbit anti-mouse Cfh (**B**) antibodies probed against increasing concentrations of human (0.05, 0.1, and 0.2 µg/ml in lanes 2–4, respectively) and mouse (0.05, 0.1, and 0.2 µg/ml in lanes 5–7, respectively) purified complement factor H, and increasing volumes of mouse serum (1, 2.5, 5.0, and 10 µl serum/lane, lanes 8–11, respectively, loaded 40 µl total volume/lane). The goat anti-mouse Cfh antibody recognized human and mouse Cfh, as well as Cfh in mouse serum (**A**), while the rabbit anti-mouse Cfh antibody recognized only mouse Cfh and Cfh in mouse serum (**B**). Nonspecific binding by secondary antibodies was tested by primary antibody deletion (Lane 12). Both antibodies used against serum (1 µl/lane) from *129/Sv Cfh*$^{-/-}$ (KO) and their wild-type background strain 129/Sv (WT) recognized Cfh only in serum from the background strain (WT) and C57BL/6 (B6) serum ran as a control (**C**). Note that both antibodies recognized only one major band at approximately 155 kDa (red arrow), the approximate weight of Cfh.

probe DapB showed no signal (Figure 4A,D). The positive control, a probe for RPE65, showed a robust signal in the RPE as expected (Figure 4B,E). The Cfh message was expressed mainly in the RPE with negligible expression in the choroid (Figure 4C,F). In addition, no message was detected in the photoreceptors (data not shown).

The results for ISH in the *Cfh* knockout mice and their background strain 129/Sv are shown in Figure 4G–N. The *Cfh* knockout mice negative and positive controls (Figure 4H,J, respectively) showed results similar to the background strain's controls (Figure 4G,I, respectively). The background strain (129/Sv) produced results similar to the C57BL/6 mouse eye with the Cfh message observed in the RPE (Figure 4K). However, the Cfh message was still detected in the RPE of the knockout (Figure 4L), albeit the signal was greatly reduced. The intensity of the signal present can be better observed when the fluorescent property of Fast Red is utilized and the sections viewed using a rhodamine filter in the background strain and the *Cfh*$^{-/-}$ (Figure 4M,N, respectively).

Antibody specificity for mouse complement factor H: Western blot analysis confirmed that the two antibodies we used in our study identified mouse complement factor H (Cfh protein; Figure 5). The goat antibody recognized the purified mouse and human CFH protein (Figure 5A), while the rabbit antibody identified only the mouse Cfh protein (Figure 5B). Both antibodies recognized the Cfh protein in mouse serum as one primary band at approximately 155 kDa, which had the same molecular weight as the purified Cfh protein run as a positive control on the same gel. Western blots performed using knockout mouse serum demonstrated a loss of the Cfh protein band, which was clearly present in the C57BL/6 (B6) and wild-type background strain (129/Sv) serum, by both antibodies (Figure 5C). Note that both antibodies detected only one major protein band of 155 kDa in serum thus demonstrating their specificity.

Complement factor H localization in the outer retina by immunohistochemistry: While ISH studies were performed to localize cells expressing mRNA, immunohistochemistry (IHC) was used to study Cfh protein distribution. The IHC results using both anti-Cfh antibodies in eye tissue from different mouse strains along with their negative controls are shown in Figure 6. The goat anti-Cfh antibody immunolabeled photoreceptor outer segments (OS) of the BALB/c mouse eye, with occasional labeling extending into the photoreceptor inner segments (IS), believed to be cone cells (Figure 6C). When the goat anti-Cfh antibody was preabsorbed with a blocking peptide, and used alongside the stock antibody in

an IHC experiment, immunolabeling was completely absent with the preabsorbed antibody (Appendix 2).

A somewhat similar immunolabeling pattern was observed with the rabbit anti-Cfh antibody labeling the OS, but patchy labeling was also observed along the apical edge of the RPE (Figure 6D). In addition, this antibody labeled the choroid and occasionally the cytoplasm of some RPE cells.

Interestingly, both antibodies produced a different pattern in the 129/Sv background strain with immunolabeling occurring in the IS, compared to the OS in the BALB/c strain (Figure 6G,K). When the Cfh knockout was immunolabeled with either antibody, a signal in the IS was still observed, but the signal intensity was markedly reduced (Figure 6H,L).

Sagittal sections of a mouse eye immunolabeled with rhodopsin (green) and the goat anti-mouse Cfh antibodies (red) showed Cfh to be centrally localized as a band in the OS, with occasional Cfh labeling observed in what is believed to be cone cell IS (white arrowheads, Figure 7A). When a sagittal eye section was immunolabeled for blue and red/green opsin antibodies (white), which label cone cells, and anti-Cfh antibody (red), a similar Cfh labeling pattern was observed (Figure 7B). However, polarized staining of Cfh and opsins was also observed. Thus, Cfh appears to be associated with rod and cone cells. To determine the location of Cfh in relation to the rod and cone photoreceptors, coronal sections from the C57BL/6 mice were used. This allowed us to acquire cross sections of rod and cone photoreceptors and to visualize the location of Cfh within both photoreceptor types. Coronal sections labeled with fluorescein conjugated WGA (labels matrix domains surrounding rod photoreceptors), and an anti-Cfh antibody clearly show Cfh labeling (red) within the rod photoreceptor outer segments (Figure 7C,D). Note that not all rod outer segments (denoted by green rings) contain Cfh internally. This confirms what is seen in the sagittal sections, since Cfh is not located throughout the rod photoreceptors (green), only in the central region of rod OS (Figure 7A). When the coronal sections were labeled with fluorescein conjugated PNA (labels cone matrix domain-green) and an anti-Cfh antibody, Cfh (red) was clearly located inside the cone cells (Figure 7E,F).

Statistical analysis: For the qPCR experiments, RNA was isolated from the RPE/choroid from six animals (biologic replicates)/group. The qPCR analysis was performed for each biologic replicate, and each biologic replicate was run in

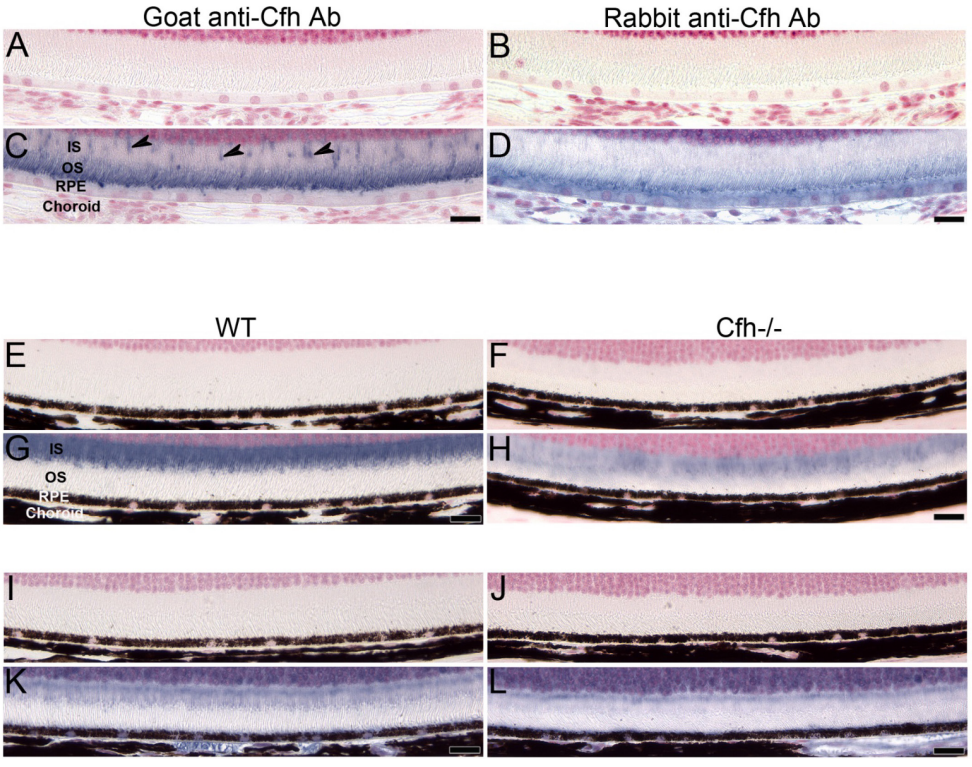

Figure 6. Immunohistochemistry for Cfh protein expression in the BALB/c, 129/Sv, and *129/Sv Cfh*$^{-/-}$ eye. A BALB/c male eye sectioned near the optic nerve labeled for Cfh using two anti-Cfh antibodies (**C**, **D**), along with its paired negative control (**A**, **B**). Goat anti-mouse Cfh antibody predominately labeled photoreceptor outer segments (OS) and what appear to be cone cell photoreceptor (arrow heads) inner segments (IS; **C**). The rabbit anti-mouse Cfh antibody labeled OS, the apical edge of the retinal pigment epithelium (RPE) cells, and only lightly labeled the RPE cytoplasm (**D**). The 129/Sv background strain eyes and *Cfh* knockout (*129/Sv Cfh* $^{-/-}$) eyes paired with their negative controls (**E**, **F**, **I**, **J**) immunolabeled with goat anti-mouse Cfh antibody (**G**, **H**) or rabbit anti-mouse Cfh antibody (**K**, **L**). Cfh labeling was observed in the *Cfh* knockout eyes (**H**, **L**) using both antibodies, but the signal was greatly reduced compared to the wild-type (WT) eyes (**G**, **K**). The residual presence of the signal could be due to cross-reactivity with Cfhr2 protein, since both antibodies recognize Cfh and Cfhr2 proteins. Scale bar=20 µm.

triplicate. Therefore, the data for each biologic group were an average of eighteen individual replicate runs. Raw qPCR data were normalized to the geometric mean of the three reference genes *Gapdh*, *B2M*, and *Hprt13*. A pairwise *t* test for statistical significance between each group was performed using a one-tailed unpaired Student's *t* test. Statistically significant differences were defined as $p<0.05$.

DISCUSSION

Our results specifically address the expression and distribution of *Cfh* and *Cfh*-related genes in the mouse RPE/choroid. We did not detect Cfhr3, Cfhr1, or Gm4788 expression in the posterior pole of the mouse eye by qPCR. Similarly, Luo et al. found Cfh in the mouse retina and RPE/choroid but not Cfhr1 using qPCR [12]. In addition, they verified the expression of Cfh but not Cfhr1 in vitro using primary cultured mouse RPE cells and a microglial cell line (BV2 cells) by qPCR [12]. In our experiments, we found clear evidence of strong Cfh expression and a low level of Cfhr2 expression.

In situ hybridization studies used an oligo probe designed to specifically detect only Cfh mRNA and not cross-react with Cfhr2. The ISH images of the outer retina (Figure 4) show that the RPE is the major source of Cfh mRNA in the outer retina. Cfh mRNA was absent in the outer nuclear layer and photoreceptors (data not shown). In situ hybridization studies in the *Cfh* knockout mouse confirmed the loss of most but not all expression of Cfh mRNA (Figure 4L,N). This low level signal in the knockout could possibly be the result of a read-through message of the knocked-out gene, and not due to cross-reactivity with other related family members, since the probe was designed specifically not to recognize Cfhr2.

In an attempt to get a clearer answer to the question of the tissue distribution of Cfh protein in the posterior pole, we developed a new freeze substitution fixation method to use with mouse-specific antibody preparations. Freeze substitution was primarily designed as a method for preparing samples for electron microscopy. Reviews of the use of this method in eye research can be found in the literature [24-26].

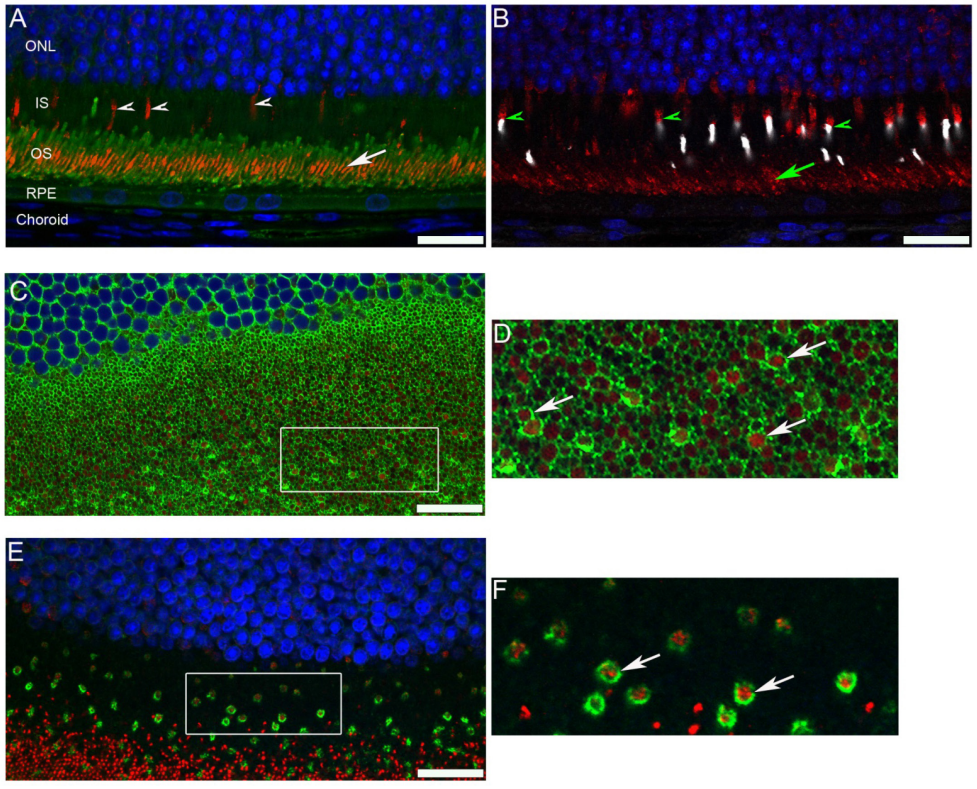

Figure 7. Cfh localization within rod and cone photoreceptors. A sagittal section from a male BALB/c mouse eye immunolabeled for rhodopsin (green), Cfh (red), and a 4',6-diamidino-2-phenylindole (DAPI) nuclear stain (blue) showed only a localized band of Cfh in the central region of the OS (white arrow), but not throughout the OS. In addition, occasional Cfh labeling of cells believed to be cone cell IS was observed (white arrowheads; **A**). A sagittal section from a male BALB/c mouse eye immunolabeled for blue and red/green opsins (white), Cfh (red), and a DAPI nuclear stain (blue) showed a similar band of Cfh in the central region of the OS (green arrow; **B**). Cone cells labeled with the opsin antibodies (green arrowheads) exhibit a polarized distribution of blue and red/green opsins (white) and Cfh (red). A coronal section from a male C57BL/6 eye double labeled with fluorescein conjugated WGA (green), which labels the matrix domains surrounding rod photoreceptors, and Cfh (red) showing Cfh within rod photoreceptor OS (**C**). The delineated area of interest is magnified and shown on the right. Cfh is clearly localized within the rods (arrows; **D**). A coronal section from a male C57BL/6 eye labeled with fluorescein conjugated PNA (green), which binds cone matrix domains, and Cfh (red) showing Cfh is clearly localized within the cone cells (arrows; **E**). The delineated area of interest is magnified and shown on the right (**F**). IS=photoreceptor inner segments; OS=outer segments; RPE=retinal pigment epithelium; WGA=wheat germ agglutinin; PNA=peanut agglutinin. Scale bar=20 µm.

In addition to this primary use, however, several newer reports have illustrated the use of freeze substitution for immunohistochemistry at the light microscopy level [27,28]. We chose this method based on its superior ability to preserve tissue morphology and antigenicity for the antibodies we used. In the mouse, alcohols and acetone have been explored for flash-freezing techniques with whole eyes, and an extension of these methods has been used for in situ cryopreservation in the living mouse [27,28]. We explored methanol/acetic acid, acetone/2% formaldehyde, and acetone/2% paraformaldehyde for freeze substitution (data not shown). The best result in terms of morphology and antigen preservation for immunohistochemistry was methanol containing 3% acetic acid as reported by Yoon and FitzGerald [29].

On the protein level, there are several reports of Cfh localization in the eye, with varying results. Kim et al., using cell culture and western blots, and Quidel's goat anti-human CFH antiserum showed that bovine and human RPE cells make and secrete Cfh and that interferon-gamma (IFN-gamma) increases Cfh production. Only weak labeling of Cfh was observed in the RPE, unless stimulated with IFN-gamma [30]. Mandal and Ayyagari also used Quidel's goat anti-human CFH antiserum on the mouse eye and observed labeling in the mouse RPE, IS, outer plexiform layer (OPL), inner plexiform layer (IPL), ganglion cell layer (GCL), and limiting membranes [13]. We attempted to purify the Quidel goat anti-human CFH antiserum using immunoaffinity columns, but after affinity purification, mouse Cfh protein immunolabeling in the mouse tissue was significantly reduced (data not shown). Chen et al. used Abcam's sheep anti-human CFH antibody, which labeled mouse RPE, Bruch's membrane, and a choroidal vessel [16]. Lyzogubov et al. also used an Abcam sheep anti-human CFH antibody that labeled only mouse RPE [17]. Von Leithner et al. used a Calbiochem goat anti-human CFH antiserum and found labeling only in Bruch's membrane of the mouse eye [14]. Liu et al. reported Cfh protein in the mouse photoreceptor sensory cilium complex [15]. Additionally, we observed strain variation in Cfh localization within photoreceptors. The only group that found results similar to ours is Amadi-Obi et al., who used a goat anti-mouse Cfh antibody. They found labeling in the mouse OS, not the RPE [31]. Our immunohistochemistry results localize the Cfh protein in photoreceptors not in the RPE. Given the antigenic differences between mouse and human complement proteins, antibodies specific for a particular species proteins should be used and cross-reactivity studies performed with western or dot blot analysis.

We purposely chose two antibodies that were produced using mouse Cfh antigens as the immunogen. The goat anti-mouse Cfh antibody was raised against a peptide (amino acids 250–300) mapping within an internal region of Cfh of mouse origin. The rabbit anti-mouse Cfh antibody was raised against amino acids 61–360 mapping within an internal region of factor H of mouse origin. In addition, the antibodies were affinity purified to help reduce non-specific binding. Each antibody's immunogen sequence was run through a BLAST search algorithm against the mouse protein database at the NCBI to test for cross-reactivity with other mouse proteins (data not shown). The BLAST results for both antibodies showed significant homology only with the Cfh and Cfhr2 (Cfhrb) proteins.

Our western blots are somewhat different from those published by other groups [11,32]. Most of these groups used sodium dodecyl sulfate (SDS) gels under oxidizing conditions. Our gels were run with reducing agent (beta mercaptoethanol), to reduce any disulfide bonds, and the blots clearly identify only one 155 kDa band equivalent to a Cfh protein monomer (Figure 5). The possibilities for additional bands on western blots from other authors may be due to cross-reactivity to other CFH-related proteins, or Cfh dimers [32].

When the Cfh knockout was immunolabeled with either antibody, a signal in the IS was still observed, but the signal intensity was markedly reduced (Figure 6H,L). Since both antibodies were produced with immunogens that share 90–95% homology with Cfhr2, it is expected that each antibody would recognize Cfhr2 protein. In addition, we observed mildly increased expression of Cfhr2 mRNA in the knockout mice (Figure 3C), which could have led to elevated Cfhr2 protein expression in the knockout mice.

The orientation of whole fixed eyes allows for the orientation of individual paraffin sections, among other benefits. Most of our images present a sagittal section near or through the optic disc. At first, we concluded that the distribution of Cfh immunolabeling was in the inferior portion of the sagittal sections. Several papers in the literature have discussed polarized distribution of gene expression and/or protein distribution between the superior and inferior regions of the mouse retina [13,33-35]. However, our work did not contain adequate positive controls to verify this finding for Cfh. Additionally, some of the authors cited used flat mounts with an orientation to give a complete view of the labeled regions.

Taken together, our results suggest that the RPE is the primary source for producing Cfh in the RPE/choroid and that the resulting protein is likely secreted into the inner photoreceptor matrix space. We have not addressed the variability in the location of Cfh within the inner photoreceptor matrix. We found evidence for Cfh labeling inside rod outer segments and inside cone cell inner segments. This topic requires more

examination with better tools to sort out the effects of Cfh transport and the possibility of its variable localization being attributed to a diurnal rhythm.

APPENDIX 1.

Mouse and human CFH genes and corresponding protein names in the literature. To access the data, click or select the words "Appendix 1."

APPENDIX 2.

To access the data, click or select the words "Appendix 2." Immunohistochemistry of a male BALB/c eye labeled using goat anti-Cfh antibody (A) and goat anti-Cfh antibody pre-absorbed with blocking peptide (B). Pre-absorbing the antibody with the blocking peptide completely eliminated the signal. Scale bar equals 20 microns. Abbreviations: inner nuclear layer (INL), outer nuclear layer (ONL), inner segments (IS), outer segments (OS), retinal pigment epithelium (RPE).

ACKNOWLEDGMENTS

Supported by NIH grants R01EY021024 and R01EY021537 to LMH and ZSM and an Unrestricted Grant from Research to Prevent Blindness to the Department of Ophthalmology, School of Medicine at University of California, Davis, and NEI Core Facilities grant P30EY012576 (UCD). Work at UC Davis was conducted in a facility constructed with support from Research Facilities Improvement Program Grant Number C06 RR-12088–01 from the National Center for Research Resources, National Institutes of Health. We thank Dr. Matthew Pickering (Imperial College London) and Dr. Gregory Hageman (University of Utah) for providing the $Cfh^{-/-}$ mice. We also thank Matthew H. Bordbari for superb technical help with RNA isolations and qPCR. Commercial interests: Zeljka Smit-McBride, none, Sharon L. Oltjen, none, Roxana A. Radu, none, Jason Estep, none, Anthony T. Nguyen, none, Qizhi Gong, none, and Leonard M. Hjelmeland, none. This data was presented in preliminary form at ARVO 2013 and 2014.

REFERENCES

1. Hageman GS, Anderson DH, Johnson LV, Hancox LS, Taiber AJ, Hardisty LI, Hageman JL, Stockman HA, Borchardt JD, Gehrs KM, Smith RJ, Silvestri G, Russell SR, Klaver CC, Barbazetto I, Chang S, Yannuzzi LA, Barile GR, Merriam JC, Smith RT, Olsh AK, Bergeron J, Zernant J, Merriam JE, Gold B, Dean M, Allikmets R. A common haplotype in the complement regulatory gene factor H (HF1/CFH) predisposes individuals to age-related macular degeneration. Proc Natl Acad Sci USA 2005; 102:7227-32. [PMID: 15870199].

2. Hageman GS, Hancox LS, Taiber AJ, Gehrs KM, Anderson DH, Johnson LV, Radeke MJ, Kavanagh D, Richards A, Atkinson J, Meri S, Bergeron J, Zernant J, Merriam J, Gold B, Allikmets R, Dean M. Extended haplotypes in the complement factor H (CFH) and CFH-related (CFHR) family of genes protect against age-related macular degeneration: characterization, ethnic distribution and evolutionary implications. Ann Med 2006; 38:592-604. [PMID: 17438673].

3. Klein RJ, Zeiss C, Chew EY, Tsai JY, Sackler RS, Haynes C, Henning AK, SanGiovanni JP, Mane SM, Mayne ST, Bracken MB, Ferris FL, Ott J, Barnstable C, Hoh J. Complement factor H polymorphism in age-related macular degeneration. Science 2005; 308:385-9. [PMID: 15761122].

4. Swaroop A, Branham KE, Chen W, Abecasis G. Genetic susceptibility to age-related macular degeneration: a paradigm for dissecting complex disease traits. Hum Mol Genet 2007; 16:R174-82. [PMID: 17911160].

5. Chen W, Stambolian D, Edwards AO, Branham KE, Othman M, Jakobsdottir J, Tosakulwong N, Pericak-Vance MA, Campochiaro PA, Klein ML, Tan PL, Conley YP, Kanda A, Kopplin L, Li Y, Augustaitis KJ, Karoukis AJ, Scott WK, Agarwal A, Kovach JL, Schwartz SG, Postel EA, Brooks M, Baratz KH, Brown WL, Brucker AJ, Orlin A, Brown G, Ho A, Regillo C, Donoso L, Tian L, Kaderli B, Hadley D, Hagstrom SA, Peachey NS, Klein R, Klein BE, Gotoh N, Yamashiro K, Ferris Iii F, Fagerness JA, Reynolds R, Farrer LA, Kim IK, Miller JW, Corton M, Carracedo A, Sanchez-Salorio M, Pugh EW, Doheny KF, Brion M, Deangelis MM, Weeks DE, Zack DJ, Chew EY, Heckenlively JR, Yoshimura N, Iyengar SK, Francis PJ, Katsanis N, Seddon JM, Haines JL, Gorin MB, Abecasis GR, Swaroop A. Genetic variants near TIMP3 and high-density lipoprotein-associated loci influence susceptibility to age-related macular degeneration. Proc Natl Acad Sci USA •••; 107:7401-6. [PMID: 20385819].

6. Klein ML, Schultz DW, Edwards A, Matise TC, Rust K, Berselli CB, Trzupek K, Weleber RG, Ott J, Wirtz MK, Acott TS. Age-related macular degeneration. Clinical features in a large family and linkage to chromosome 1q. Arch Ophthalmol 1998; 116:1082-8. [PMID: 9715689].

7. Aguirre GD, Yashar BM, John SK, Smith JE, Breuer DK, Hiriyanna S, Swaroop A, Milam AH. Retinal histopathology of an XLRP carrier with a mutation in the RPGR exon ORF15. Exp Eye Res 2002; 75:431-43. [PMID: 12387791].

8. Ramkumar HL, Zhang J, Chan CC. Retinal ultrastructure of murine models of dry age-related macular degeneration (AMD). Prog Retin Eye Res •••; 29:169-90. [PMID: 20206286].

9. Ramkumar HL, Zhang J, Chan CC. Retinal ultrastructure of murine models of dry age-related macular degeneration (AMD). Prog Retin Eye Res 2010; 29:169-90. [PMID: 20206286].

10. Ufret-Vincenty RL, Aredo B, Liu X, McMahon A, Chen PW, Sun H, Niederkorn JY, Kedzierski W. Transgenic mice

expressing variants of complement factor H develop AMD-like retinal findings. IOVS 2014.

11. Hellwage J, Eberle F, Babuke T, Seeberger H, Richter H, Kunert A, Hartl A, Zipfel PF, Jokiranta TS, Jozsi M. Two factor H-related proteins from the mouse: expression analysis and functional characterization. Immunogenetics 2006; 58:883-93. [PMID: 17028856].
12. Luo C, Chen M, Xu H. Complement gene expression and regulation in mouse retina and retinal pigment epithelium/choroid. Mol Vis 2011; 17:1588-97. [PMID: 21738388].
13. Mandal MN, Ayyagari R. Complement factor H: spatial and temporal expression and localization in the eye. Invest Ophthalmol Vis Sci 2006; 47:4091-7. [PMID: 16936129].
14. Lundh von Leithner P, Kam JH, Bainbridge J, Catchpole I, Gough G, Coffey P, Jeffery G. Complement factor h is critical in the maintenance of retinal perfusion. Am J Pathol 2009; 175:412-21. [PMID: 19541934].
15. Liu Q, Tan G, Levenkova N, Li T, Pugh EN Jr, Rux JJ, Speicher DW, Pierce EA. The proteome of the mouse photoreceptor sensory cilium complex. Molecular & cellular proteomics MCP 2007; 6:1299-317. [PMID: 17494944].
16. Chen M, Forrester JV, Xu H. Synthesis of complement factor H by retinal pigment epithelial cells is down-regulated by oxidized photoreceptor outer segments. Exp Eye Res 2007; 84:635-45. [PMID: 17292886].
17. Lyzogubov VV, Tytarenko RG, Jha P, Liu J, Bora NS, Bora PS. Role of ocular complement factor H in a murine model of choroidal neovascularization. Am J Pathol 2010; 177:1870-80. [PMID: 20813971].
18. Smit-McBride Z, Oltjen SL, Lavail MM, Hjelmeland LM. A strong genetic determinant of hyperoxia-related retinal degeneration on mouse chromosome 6. Invest Ophthalmol Vis Sci 2007; 48:405-11. [PMID: 17197561].
19. Wang F, Flanagan J, Su N, Wang LC, Bui S, Nielson A, Wu X, Vo HT, Ma XJ, Luo Y. RNAscope: a novel in situ RNA analysis platform for formalin-fixed, paraffin-embedded tissues. The Journal of molecular diagnostics JMD 2012; 14:22-9. [PMID: 22166544].
20. Józsi M, Zipfel PF. Factor H family proteins and human diseases. Trends Immunol 2008; 29:380-7. [PMID: 18602340].
21. Fritsche LG, Lauer N, Hartmann A, Stippa S, Keilhauer CN, Oppermann M, Pandey MK, Kohl J, Zipfel PF, Weber BH, Skerka C. An imbalance of human complement regulatory proteins CFHR1, CFHR3 and factor H influences risk for age-related macular degeneration (AMD). Hum Mol Genet 2010; 19:4694-704. [PMID: 20843825].
22. Vik DP, Munoz-Canoves P, Kozono H, Martin LG, Tack BF, Chaplin DD. Identification and sequence analysis of four complement factor H-related transcripts in mouse liver. J Biol Chem 1990; 265:3193-201. [PMID: 1689298].
23. Pickering MC, Cook HT, Warren J, Bygrave AE, Moss J, Walport MJ, Botto M. Uncontrolled C3 activation causes membranoproliferative glomerulonephritis in mice deficient in complement factor H. Nat Genet 2002; 31:424-8. [PMID: 12091909].
24. Meissner DH, Schwarz H. Improved cryoprotection and freeze-substitution of embryonic quail retina: a TEM study on ultrastructural preservation. J Electron Microsc Tech 1990; 14:348-56. [PMID: 2332811].
25. Yang Z, Stratton C, Francis PJ, Kleinman ME, Tan PL, Gibbs D, Tong Z, Chen H, Constantine R, Yang X, Chen Y, Zeng J, Davey L, Ma X, Hau VS, Wang C, Harmon J, Buehler J, Pearson E, Patel S, Kaminoh Y, Watkins S, Luo L, Zabriskie NA, Bernstein PS, Cho W, Schwager A, Hinton DR, Klein ML, Hamon SC, Simmons E, Yu B, Campochiaro B, Sunness JS, Campochiaro P, Jorde L, Parmigiani G, Zack DJ, Katsanis N, Ambati J, Zhang K. Toll-like receptor 3 and geographic atrophy in age-related macular degeneration. N Engl J Med 2008; 359:1456-63. [PMID: 18753640].
26. Buser C, Walther P. Freeze-substitution: the addition of water to polar solvents enhances the retention of structure and acts at temperatures around −60 degrees C. J Microsc 2008; 230:268-77. [PMID: 18445157].
27. Ohno N, Terada N, Saitoh S, Zhou H, Fujii Y, Ohno S. Recent development of in vivo cryotechnique to cryobiopsy for living animals. Histol Histopathol 2007; 22:1281-90. [PMID: 17647200].
28. Terada N, Ohno N, Saitoh S, Saitoh Y, Ohno S. Immunoreactivity of glutamate in mouse retina inner segment of photoreceptors with in vivo cryotechnique. J Histochem Cytochem 2009; 57:883-8. [PMID: 19471014].
29. Yoon KH, FitzGerald PG. Periplakin interactions with lens intermediate and beaded filaments. Invest Ophthalmol Vis Sci 2009; 50:1283-9. [PMID: 19029034].
30. Kim YH, He S, Kase S, Kitamura M, Ryan SJ, Hinton DR. Regulated secretion of complement factor H by RPE and its role in RPE migration. Graefe's archive for clinical and experimental ophthalmology = Albrecht Von Graefes Arch Klin Exp Ophthalmol 2009; 247:651-9. .
31. Amadi-Obi A, Yu CR, Dambuza I, Kim SH, Marrero B, Egwuagu CE. Interleukin 27 induces the expression of complement factor H (CFH) in the retina. PLoS ONE 2012; 7:e45801-[PMID: 23029250].
32. Goicoechea de Jorge E, Caesar JJ, Malik TH, Patel M, Colledge M, Johnson S, Hakobyan S, Morgan BP, Harris CL, Pickering MC, Lea SM. Dimerization of complement factor H-related proteins modulates complement activation in vivo. Proc Natl Acad Sci USA 2013; 110:4685-90. [PMID: 23487775].
33. Corbo JC, Myers CA, Lawrence KA, Jadhav AP, Cepko CL. A typology of photoreceptor gene expression patterns in the mouse. Proc Natl Acad Sci USA 2007; 104:12069-74. [PMID: 17620597].
34. Coffey PJ, Gias C, McDermott CJ, Lundh P, Pickering MC, Sethi C, Bird A, Fitzke FW, Maass A, Chen LL, Holder GE, Luthert PJ, Salt TE, Moss SE, Greenwood J. Complement factor H deficiency in aged mice causes retinal abnormalities and visual dysfunction. Proc Natl Acad Sci USA 2007; 104:16651-6. [PMID: 17921253].

35. Szél A, Rohlich P, Caffe AR, Juliusson B, Aguirre G, Van Veen T. Unique topographic separation of two spectral classes of cones in the mouse retina. J Comp Neurol 1992; 325:327-42. [PMID: 1447405].